Therapeutic proton beams: LET, RBE and microdosimetric spectra with gas and silicon detectors.

P.Colautti[1], A. Bianchi [1,2,3], A. Selva[1], D. Bortot[4,5], D. Mazzucconi [4,5], A. Pola [4,5], S. Agosteo [4,5], G. Petringa[6], G. A. P. Cirrone [6], V. Conte[1]

[1] *Istituto Nazionale di Fisica Nucleare INFN, Laboratori Nazionali di Legnaro, viale dell'Università 2, Legnaro (Padova), Italy*
[2] *Belgian Nuclear Research Centre, SCK•CEN, Boeretang 200, 2400 Mol, Belgium*
[3] *UHasselt, Faculty of Engineering Technology, Centre for Environmental Sciences, Nuclear Technology Centre, Agoralaan, 3590 Diepenbeek, Belgium*
[4] *Istituto Nazionale di Fisica Nucleare INFN, Sezione di Milano, via Celoria 16, Milano, Italy*
[5] *Politecnico di Milano, Dipartimento di Energia, via La Masa 34, Milano, Italy*
[6] *Istituto Nazionale di Fisica Nucleare INFN, Laboratori Nazionali del Sud, via Santa Sofia 62, Catania, Italy*

***Corresponding author**: Paolo Colautti, paolo.colautti@lnl.infn.it*

Abstract

A sealed mini-TEPC able to work in gas-steady modality, a monolithic silicon device composed by a matrix of micrometric cylindrical diodes and a residual energy measurement stage and the silicon MicroPlus Bridge detector were used to perform microdosimetric measurements at the 62 MeV proton clinical SOBP of CATANA at the Southern National Laboratories of INFN (LNS – INFN, Catania, Italy). Measurements were taken at the same different positions in a PMMA phantom, in order to analyse the detector response differences.
Finally, a weighting function was applied to the spectra to see if the microdosimetric detectors are able to monitor RBE data for glioma cells (U87) irradiated at six positions along the same modulated 62-MeV proton beam. The results obtained with the three microdosimeters are compared and discussed.

Keywords: Microdosimetry; Proton therapy; Proton RBE; mini-TEPC; Silicon telescope detector; MicroPlus Bridge detector.

1. Introduction

Proton therapy is a cancer treatment technique that uses accelerated protons to treat tumours, instead of photons and electrons employed in conventional radiotherapy.
When protons are used, the physical dose has to be weighted for the corresponding Relative Biological Effectiveness (RBE) to take into account the different effect of proton radiation field on cells as compared to photons, for the same absorbed dose. In proton therapy a fixed RBE equal to 1.1 is used for all treatment depths. However, an increasing RBE, reaching up to 1.7 in the fall-off of the SOBP, was found in several biological assays [1].
It has been demonstrated that the effectiveness of a radiotherapy treatment is mainly related to the local pattern of energy deposition at the subcellular level. More clustered energy-deposition

patterns result in lesions that are more difficult for the cell to repair [2]. On average, this physical situation happens when the linear density of the energy transferred (LET) is relatively higher. However, a LET detector does not yet exist, while small microdosimetric detector able to work in the intense therapeutic ion beams are already operative, although not commercial yet. Microdosimetric detectors measure the distribution of the energy imparted $\boldsymbol{\varepsilon_I}$ by a single particle in a microscopic volume. The ratio of $\boldsymbol{\varepsilon_I}$ to the detector sensitive-volume equivalent mean-chord length $\bar{l}$ gives the mean linear-energy density of the particle (measured with the detector size resolution), which is called "lineal energy $\boldsymbol{y}$". Microdosimetric measurements can be performed with gas counters [3], namely miniaturized tissue-equivalent gas-proportional counters (mini-TEPC) of 1 µm of equivalent size, with thin silicon detectors of 1-2 µm thickness [4], with thick silicon detectors of 10 µm or larger thickness like the Bridge microdosimeter [5] and with 2 µm-thick diamond detectors [6]. Mini-TEPCs have already shown to be able to monitor the dose-averaged LET of a clinical proton beam with good accuracy [3]. They have also shown to be capable to directly monitor the RBE of clinical protons beam [7]. The Silicon telescope detector had already measured in a clinical proton beam, being its microdosimetric spectra consistent with mini-TEPC spectra collected years before in a similar proton beam [8].
In this work, the mini-TEPC and the two silicon detectors have been placed in same positions in the proximal edge, in the SOBP and in the distal edge of the same CATANA therapeutic beam, in order to accurately compare the three detector responses and to better establish their differences. Moreover, the dose distributions *d(y)* measured by the three detectors have been weighted with the Loncol weighting function [9], (similarly to what was done in reference 7) in order to investigate the detectors' ability to monitor the RBE values, which had previously been measured in the same facility and in the same phantom positions.

2. Materials and Methods

2.1 The sealed mini-TEPC: detector and data processing

FIGURE 1

Figure 1. The mini-TEPC cross section. Green area: sensitive volume. Red area: A-150 plastic. Yellow area: Rexolite®. Grey area: titanium.

The mini-TEPC is a gas counter with a sensitive volume of only 0.9 mm in diameter and height (the green area of figure 1) to cope with high intensity beams such as those employed in hadron therapy. The mini-TEPC of figure 1 was designed to work in gas flow modality, in order to have stable responses even after rapid changes in pressure. The detector used in this work is a modified version of the one shown in figure 1, which can operate in gas steady modality [3]. The detector sensitive volume is surrounded by a 0.35 mm–thick A150–cathode wall, a 0.35 mm Rexolite® insulator, and a 0.2 mm–thick titanium sleeve, giving a total external diameter of 2.7 mm. The detector wall total-thickness is equivalent to 1.37 mm of liquid water in terms of energy loss (calculated by taking into account the average stopping–power ratio of the different materials in

the proton energy range from 0 MeV to 62 MeV). After an optimized cleaning and filling procedure, the detector was filled with 45.4 kPa of propane and sealed. The gas sensitive-volume thickness corresponds to a site size of 0.75 µm in pure propane with density 1 g/cm³, which is equivalent, in term of imparted energy, to 0.85 µm of liquid water in the proton energy range used.
The mini-TEPC measurements were performed biasing the cathode at -700 V and keeping the anode grounded through the pre-amplifier. The high gas gain and the low noise conditions allowed for acquiring lineal energy events down to 0.4 keV/µm. The pulse spectrum has been calibrated in lineal energy y by fitting the proton edge with a Fermi-like function [8] and assigning to the inflection point the value of 143 keV/µm. This value has been calculated by using the SRIM look up tables [11]. The maximum lineal energy value in propane gas, 162 keV/µm, has been multiplied by the mean ratio $dE/dx_{water} / dE/dx_{propane}$, namely 0.88.
The frequency spectra $f(y)$ were linearly fitted between 0.4 and 0.5 keV/µm and extrapolated down to the y value of 0.01 keV/µm.

2.2 The silicon telescope: detector and data processing

As thin silicon detector, the silicon telescope was used. The device consists of a ΔE and an E stage. The ΔE stage is composed by a matrix of micrometric cylindrical diodes of 1.9 µm of thickness and 9 µm of diameter. The E stage is 500 µm thick. E and ΔE stages are fabricated on a single silicon substrate and separated by a deeply implanted p+ cathode [4]. The E stage, biased at 150 V, records the residual energy of the incident protons emerging from the ΔE stage, which is biased at 9 V, when the residual proton range is less than the E stage thickness (i.e., for protons of less than 8 MeV of energy). The calibration of the measured spectra in terms of energy imparted ε_1 was performed using a calibrated pulse generator. In turn, the pulser was calibrated using a fully depleted PIN diode of capacitance similar to that of the silicon telescope, which collects charge corresponding to the total energy of alpha particles from a sealed ^{244}Cm source (5.18 MeV of mean energy). More details about the calibration procedure are in reference 12.

The water-equivalent correction was performed on the lineal energy spectra. In the distal region where protons stop completely in the E stage (thus permitting the knowledge of the impinging proton energy) the lineal energy in silicon is corrected to lineal energy in water by using the ratio $(dE/dx)_{Water} / (dE/dx)_{silicon}$ at the specific proton energy. For higher energy protons, an average ratio value of 0.58 was adopted for all the events. Here, the water-equivalent thickness, corresponding to the same energy imparted in 1.9 µm of silicon, is therefore 1.9/0.58 = 3.3 µm. The mean chord length of the sensitive volume is assumed to be its water-equivalent thickness.

The microdosimetric spectra obtained from the silicon telescope in the ΔE stage were analysed using the procedure explained in [4]. The frequency spectra have been extrapolated down to the y value of 0.01 keV/µm with a linear best-fit of data between 8 and 8.5 keV/µm.

2.3 The silicon MicroPlus Bridge probe: detector and data processing

As thick silicon detector, the MicroPlus Bridge detector was used. It was developed at CMRP at the University of Wollongong, Australia [13]. The detector is fabricated using silicon-on-insulator (SOI) wafers with 10 µm thick silicon active volume [5,14]. The detector is biased at 12 V. Charge pulses have been amplified and digitized with the multi-channel analyser (MCA) model easy-MCA (ORTEC). The setting was 8962 channels for 0–10 V range. Calibration of MCA channel number to energy was performed using a calibrated pulse generator. The pulse generator had been preventively energy-calibrated by using the same sealed ^{244}Cm alpha source of 5.18 MeV of mean energy that was used to calibrate the silicon telescope. Monte Carlo simulations have pointed out that the mean $\boldsymbol{\varepsilon_I}$ value in the 10 µm silicon detector is equal to $\boldsymbol{\varepsilon_I}$ in 17.24 µm of striated muscle [15,16], which is consistent with the 0.58 factor used also for the silicon telescope. Therefore, the Bridge-detector sensitive volume is said to be equivalent to 17.24 µm of striated muscle. We have assumed the same value for liquid water equivalence, since the mean stopping powers in the energy range of CATANA beam in H_2O and in striated muscle differ by less than 2%. The mean chord length of the Bridge detector is assumed to be equal to its water-equivalent thickness.

The frequency spectra have been extrapolated down to the $\boldsymbol{y}$ value of 0.01 keV/µm with a linear best-fit of data between 0.50 and 0.55 keV/µm.

2.4 The irradiation set-up

The three detectors were irradiated in the CATANA beam line at the LNS – INFN, which uses 62 MeV proton beam and a passive half-modulated SOBP to treat ocular melanomas [17].
The beam dosimetry was performed in the standard way, by using a Markus plane parallel ion chamber, model 23343. Measurements were performed in different positions in the proximal edge, in the SOBP and in the distal edge by placing PMMA layers of different thickness between the beam and the detectors. The detector position in air (in the clinical beam iso-center) has an uncertainty of 0.15 mm (~ 0.15 µm in the water-equivalent phantom). However, since the PMMA layers had a thickness uncertainty, we have assessed a total PMMA-depth uncertainty of 0.3 mm for all the detectors at all the depths. Eventually, PMMA layers were converted in in water layers applying the factor of 1.16 ± 0.03, which has been determined as the average stopping power ratio of protons with the energies of CATANA facility, calculated by using SRIM [11].

2.5 Data processing

The frequency spectra $\boldsymbol{f(y)}$ in liquid water of all the detectors have been transformed in dose spectra $\boldsymbol{d(y)}$ and then plotted as the dimensionless quantity $\boldsymbol{yd(y)}$ against $\boldsymbol{log(y)}$. This representation makes the spectra details more visible, preserving the physical meaning. Namely, the visual area under the curve in a given $\boldsymbol{log(y)}$ interval is proportional to the relative contribution to the absorbed dose of events in that interval [18]. The mean $\boldsymbol{y}$ value of events weighted with their contribution to the dose is called dose-mean $\boldsymbol{y}$ value $\boldsymbol{\overline{y}_D}$.

The ***d(y)*** spectrum can be further weighted with a biological response function ***r(y)***, which points out the expected biological effect due to the dose component with lineal energy ***y***. We have used the Loncol's response function for mouse crypt-cell regeneration after a 8 Gy dose [9], which had already predicted good ***RBE*** values for clinical proton beams [7]. The ***r(y)*** function was extracted by comparing the ***d(y)*** spectra, collected with a spherical TEPC of 2 µm of tissue-equivalent size, in gamma, proton and neutron fields and the RBE values collected in the same fields. The microdosimetric assessment of the CATANA ***RBE*** value at a given depth, where the ***d(y)*** spectrum had been measured, has been called $\boldsymbol{RBE_{micros}}$ and calculated with the equation 1. The $\boldsymbol{RBE_{micros}}$ relative uncertainty, mainly due to the ***y*** calibration uncertainty, has been assessed to be less than 5% [7].

$$RBE_{micros} = \int_{0.01}^{y_{max}} r(y) \cdot d(y) \cdot dy \qquad (1)$$

3. Results and discussion

3.1 The spectra physical meaning

FIGURE 2a and FIGURE 2b

Figure 2. Microdosimetric spectra in liquid water collected by the three detectors: a) at the end of the distal edge; b) at the end of the SOBP. The black dot in relative dose curve represents the detector position in the water-equivalent phantom, which has 0.3 mm of uncertainty (inside the symbol size). The vertical green lines in the silicon-telescope curve point out the extrapolated data.

Figure 2, shows the microdosimetric spectra in liquid water of the three detectors in the distal edge (left side) and at the SOBP end (right side). The vertical green lines in the figure represent the extrapolated data in the silicon telescope spectra. The extrapolated data of other two detectors are not visible in the figure. All the spectra are characterized by a sharp fall of counts, called edge, at high ***y*** values and by a large peak. In order to understand the physical meaning of these two structures, it is necessary to remember that ***y*** is the ratio of the energy imparted by a single particle $\boldsymbol{\varepsilon_I}$ and the sensitive-volume mean-chord equivalent length. Therefore, detectors of different size and shape have different microdosimetric spectra in the same radiation field. However, if all the charged particles crossing the detector have ranges bigger than the sensitive volume thickness, the maximum possible ***y*** value always corresponds to the maximum ion stopping power in detector material, which in the paper has been scaled to liquid water. Conversely, if, the sensitive-volume equivalent size is larger than low-energy proton range (in particular those that have the maximum stopping-power value), then the maximum energy imparted to sensitive volume is due to those protons (necessary of higher energy) that stop exactly at the end of the sensitive volume. In this last case the proton edge has lower value. In the distal edge and at the end of the SOBP, where low energy protons populate the radiation field, the mini-TEPC and the silicon telescope show the same proton edge value, since the TEPC diameter is shorter than the range of protons at maximum stopping power and the y value for the silicon telescope is correct on an event by event basis according to the energy of the impinging proton.

On the contrary, being the Bridge detector thickness larger, the low-energy protons stop inside to the detector and the correction event by event is not available. The maximum imparted energy is due to 750 keV protons (SRIM), the range of which matches the Bridge 10 µm thickness. Therefore, the proton edge is expected to have the value of about 43 keV/µm, which is consistent with the Bridge specra shown in figure 2.
Another common characteristic of all the spectra is the large peak that appears at intermediate y values. It is located at about 20 and 10 keV/µm in the distal edge and at the end of SOBP peak (see figure 2a and 2b) and at 2.5 and 1 keV/µm in the SOBP and at the beam entrance (see figure 3a and 3b). It is due to protons that contribute more to the absorbed dose in water. Therefore, we can say that the main contribution to the absorbed dose in the different positions is due, approximately, to protons of about 1.5, 4, 20, and 62 MeV, respectively.

FIGURE 3a and Figure 3b

Figure 3. Microdosimetric spectra in liquid water collected by the mini-TEPC and by the Bridge detector: a) at the middle of the SOBP; b) at the beam entrance. The black dot in relative dose curve represents the detector position in the water-equivalent phantom, which has 0.3 mm of uncertainty (inside the symbol size). The vertical lines in the ***yd(y)*** curves point out the extrapolated data.

In figure 3, which shows microdosimetric spectra of the mini-TEPC and Bridge detector in the SOBP and at the beam entrance, the majority of ***y*** events have size less than 8 keV/µm, too small to be detected by the silicon telescope, the spectra of which are therefore not plotted. The proton edge is only barely visible in the SOBP spectra.

At beam entrance and in the SOBP, the mini-TEPC and the Bridge detector spectra show some counts of high ***y*** value. They are possible due to the target nucleus break-up, the fragments of which have high ***dE/dx*** values.

In figure 2 and 3, it is noticeable that the Bridge detector spectra are narrower than the spectra of the other detectors. That because the energy straggling in the Bridge-detector sensitive volume is smaller, because of its bigger volume.

3.2 The RBE assessment

RBE_{micros} has been calculated by using equation (1) and the dose probability density ***d(y)*** measured with the three detectors. The shape of the Loncol's biological weighting function ***r(y)*** is shown in Figure 4a. Figure 4b shows the resulting RBE_{micros} values at different depths across the proton SOBP. The Figure shows also the RBE_{10} for human glioma (U87) cells irradiated at 6 depth positions along the same modulated therapeutic proton beam. 10% uncertainty was estimated for the biological data and 5% uncertainty for the physical measurements. It is clear from Figure 4.b that in the distal region of the Bragg peak all the three microdosimeters allow for a microdosimetric ***RBE*** assessment that is in agreement with direct radiobiological measurements within estimated uncertainties. In the proximal region there is a slightly better agreement for the

mini-TEPC derived data, while the Bridge detector data are a bit lower than radiobiological data and the silicon telescope data are not available.

FIGURE 4a and FIGURE 4b

Figure 4. a): the Loncol's biological weighting function ***r(y)***. b): $\boldsymbol{RBE_{10}}$ (radiobiological data at 10% of survival) for U87 glioma cells measured at the same CATANA proton SOBP [18] and $\boldsymbol{RBE_{micros}}$ measured at different water depth with the three different microdosimeters. The dashed red line points out the therapeutic RBE value of 1.1. Estimated uncertainties are 10% for the biological data and 5% for the physical data.

It's worth observing that the Loncol's biological weighting function ***r(y)*** has been applied also to the Bridge detector, even if the sensitive volume of this device is significantly larger than the 2 μm from which the ***r(y)*** function was derived, resulting in different microdosimetric distributions as discussed in Figures 2 and 3. In spite of that, the application of the Loncol's biological weighting function to the ***d(y)*** distributions measured with the Bridge detector still leads to an acceptable assessment of the RBE, in particular in the distal region of the SOBP.

5. Conclusions

A tissue-equivalent gas-proportional counter (the mini-TEPC), a thin silicon counter (the silicon telescope) and a thick silicon counter (the Bridge detector) have measured in the CATANA therapeutic beam at several depth positions in a water-equivalent phantom.

The mini-TEPC and the thick silicon counter can measure all across the SOBP, whereas the thin silicon telescope allows for significant measurements in the distal edge only.

The Loncol's weighting function has been applied to the measured dose probability densities ***d(y)***, in order to derive a physical assessment of the biological effectiveness of the therapeutic beam. The resulting $\boldsymbol{RBE_{micros}}$ values were compared with each other and with $\boldsymbol{RBE}_{10}$ for human glioma (U87) cells irradiated at different positions across the same SOBP. Even if the Loncol's function was derived from a different biological end point, and also from microdosimetric distributions measured with a different detector (a spherical TEPC), the resulting $\boldsymbol{RBE_{micros}}$ values are all in satisfactory agreement with the biological data, when uncertainties are taken into account.

Acknowledgements

This work was supported by the 5th Scientific Commission of the Italian Institute for Nuclear Physics (INFN).

References

[1] Paganetti H., *Relative Biological Effectiveness (RBE) values for proton beam therapy. Variations as a function of biological endpoint, dose, and linear energy transfer.* Phys Med Biol 59(22), R419–72, 2014.

[2] Ward J. F. *Biochemistry of DNA Lesions,* Radiat Res 104 (2s), S103-S111, 1985.

[3] Conte V., Bianchi A., Selva A., Petringa G., Cirrone G. A. P., Parisi A., Vanhavere F., Colautti P. *Microdosimetry at the CATANA 62 MeV proton beam with a sealed miniaturized TEPC*. Phys Med 62, 114-122, 2019.

[4] Agosteo S., Fallica P.G., Fazzi, A., Introini M.V., Pola A., Vulva G. A pixelated silicone telescope for solid state microdosimetry. Radiat.Meas. 43, 585-589, 2008.

[5] Tran L. T., Prokopovich D. A., Petasecca M.,Lerch M. L. F., Kok A., Summanwar A., Hansen T. E., Da Via C., Reinhard M. I., Rosenfeld A. B. *3D radiation detectors: charge collection characterisation and applicability technology for microdosimetry.* IEEE Transactions on nuclear science 61, 1537-1543, 2014.

[6] Magrin G., Verona C., Ciocca M., Marinelli M., Mastella E., Stock M., Verona-Rinati G. *Microdosimetric characterization of clinical carbon-ion beams using synthetic diamond detectors and spectral conversion methods*. Med.Phys. 47, 713-721, 2020.

[7] L.De Nardo, V.Cesari, N.Iborra, V.Conte, P.Colautti, J.Héreault, G.Tornielli, P.Chauvel. *Microdosimetric Assessment of Nice Therapeutic Proton Beam Biological Quality.* Physica Medica XX, 71-77 (2004).

[8] S. Agosteo, G.A.P. Cirrone, P. Colautti, G. Cuttone, G. D'Angelo, A. Fazzi, M.V. Introini, D. Moro, A. Pola , V. Varoli. *Study of a silicon telescope for solid state microdosimetry: Preliminary measurements at the therapeutic proton beam line of CATANA*. Radiat. Meas. 45, 1284-1289 (2010).

[9] Loncol T., Cosgrove V., Denis J. M., Gueulette J., Mazal A., Menzel H. G., Pihet P., Sabattier R., *Radiobiological effectiveness of radiation beams with broad LET spectra: microdosimetric analysis using biological weighting functions.* Radiat Prot Dosim. 52, 347-352, 1994.

[10] Conte V., Moro D., Grosswendt B., Colautti P. *Lineal energy calibration of mini tissue equivalent gas-proportional counters (TEPC).* Multidisciplinary Applications of Nuclear Physics with Ion Beams (ION BEAMS '12) – AIP Conf. Proc. 1530, 171-178, 2013.

[11] Ziegler J.F., Ziegler M.D., Biersack J.P. *SRIM The stopping and range of ions in matter*, Nucl Instr Meth B 268, 1818–1823, 2010.

[12] Bortot D., Pola A., Agosteo S., Pasquato S., Introini M.V., Colautti P., Conte V. *A miniaturazed alpha spectrometer for the calibration of an avalanche-confinement TEPC*. Radiat. Meas. 106, 531-537, 2017.

[13] Rosenfeld A. *Novel detectors for silicon based microdosimetry, their concepts and applications.* Nucl Instrum Methods Phys Res A. 809,156–170, 2016.

[14] Tran L. T., Chartier L., Bolst D., Prokopovich D., Guatelli S., Petasecca M., Lerch M., Reinhard M., Perevertaylo V., Jackson M., Matsufuji N., Hinde D., Dasgupta M., Stuchbery A. and Rosenfeld A. B. *3D silicon microdosimetry and RBE study using 12C ion of different energies.* IEEE Trans Nucl Sci. 62, 3027–3033, 2015.

[15] Guatelli S., Reinhard M. I., Mascialino B., et al. *Tissue equivalence correction in silicon microdosimetry for protons characteristic of the LEO space environment*. IEEE Trans Nucl Sci. 55, 6, 2008.

[16] Bolst D., Guatelli S., Tran L. T., Chartier L., Lerch M. L., Matsufuji N., Rosenfeld A.B. *Correction factors to convert micro-dosimetry measurements in silicon to tissue in 12C ion therapy*. Phys Med Biol. 62, 2055–2069, 2017.

[17] Cirrone G.A.P., Cuttone G., Lojacono P. A., Lo Nigro S., Mongelli V., Patti I. V., Privitera G., Raffaele L., Rifuggiato D., Sabini M. G., Salamone V., Spatola C., Valastro L. M. *A 62-MeV proton beam for the treatment of ocular melanoma at Laboratori Nazionali del Sud-INFN,* IEEE Transactions on Nuclear Science 51(3), 860-865, 2004.

[18] International Commission on Radiation Units and Measurement (ICRU), *Microdosimetry*, Report 36, 1983.

[19] Chaudhary P., Marshall T. I., Perozziello F. M., Manti L. , Currell F. J., Hanton F., McMahon S. J., Kavanagh J. N., Cirrone G. A. P., Romano F., Prise K. M., Schettino G. *Relative Biological Effectiveness Along Monoenergetic and Modulated Bragg Peaks of a 62-MeV Therapeutic Proton Beam: A Preclinical Assessment,* Int J Radiat Oncol Biol Phys 90 (1), 27-35, 2014.

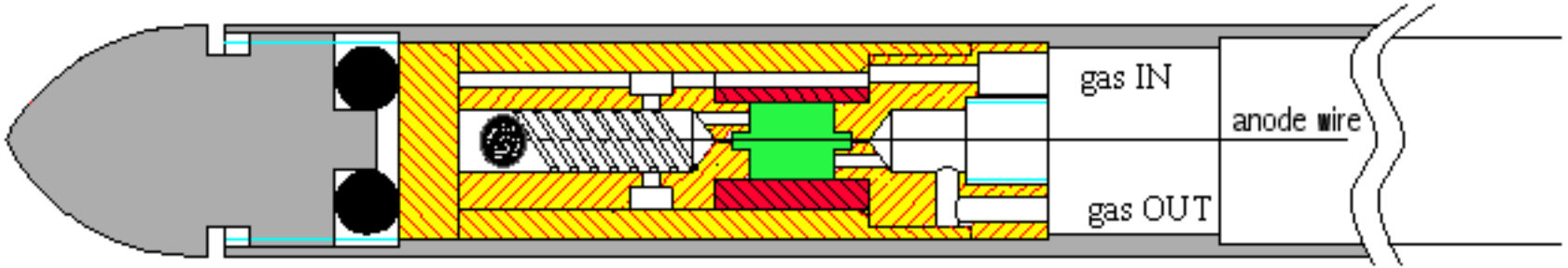
gas IN
anode wire
gas OUT

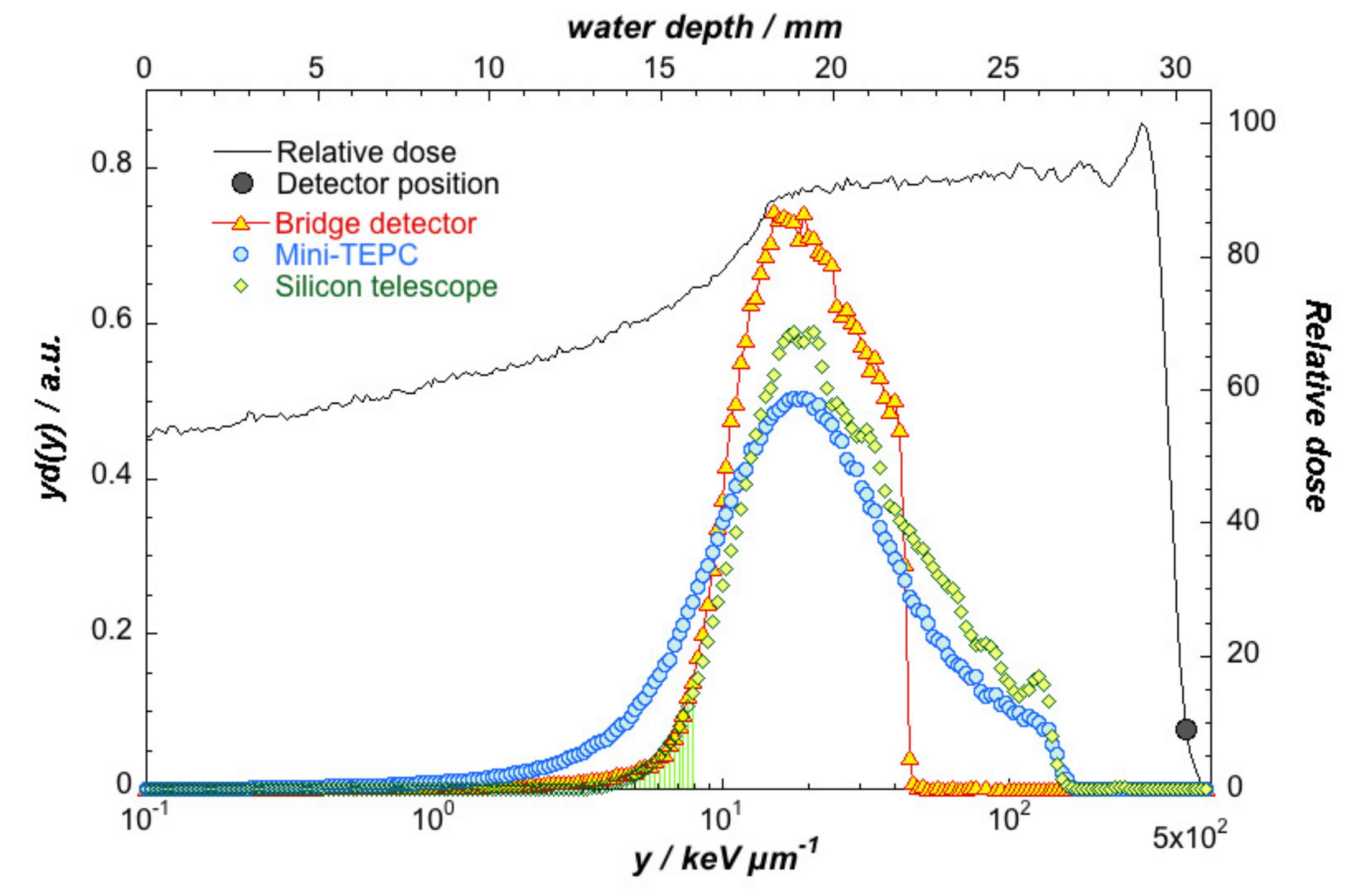
water depth / mm
0
5
10
15
20
25
30
Relative dose
Detector position
Bridge detector
Mini-TEPC
Silicon telescope
yd(y) / a.u.
0
0.2
0.4
0.6
0.8
Relative dose
0
20
40
60
80
100
10^{-1}
10^{0}
10^{1}
10^{2}
$5x10^{2}$
y / keV μm^{-1}

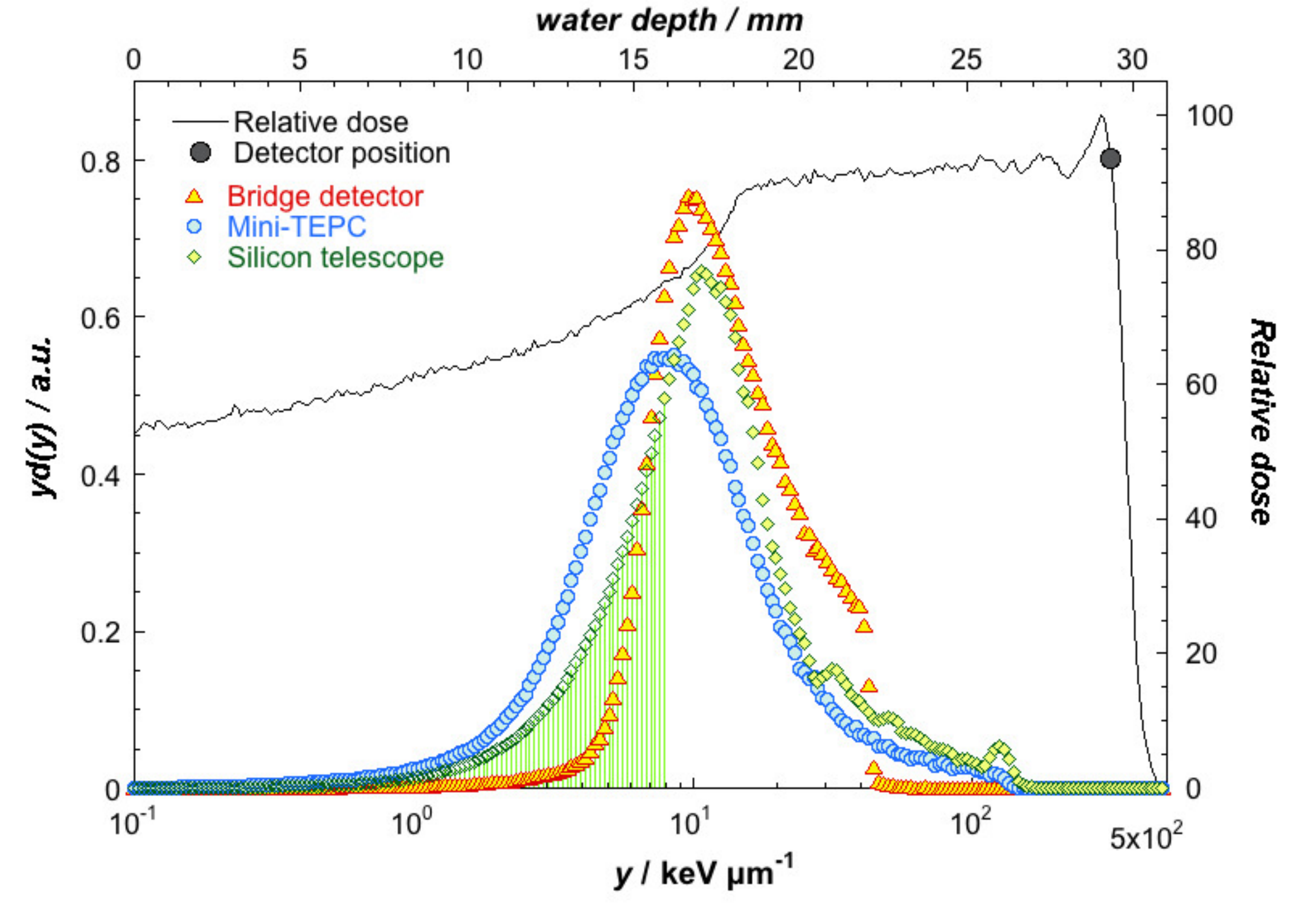
water depth / mm
0
5
10
15
20
25
30
Relative dose
Detector position
Bridge detector
Mini-TEPC
Silicon telescope
0.8
0.6
0.4
0.2
0
yd(y) / a.u.
100
80
60
40
20
0
Relative dose
10^-1
10^0
10^1
10^2
5x10^2
y / keV µm^-1

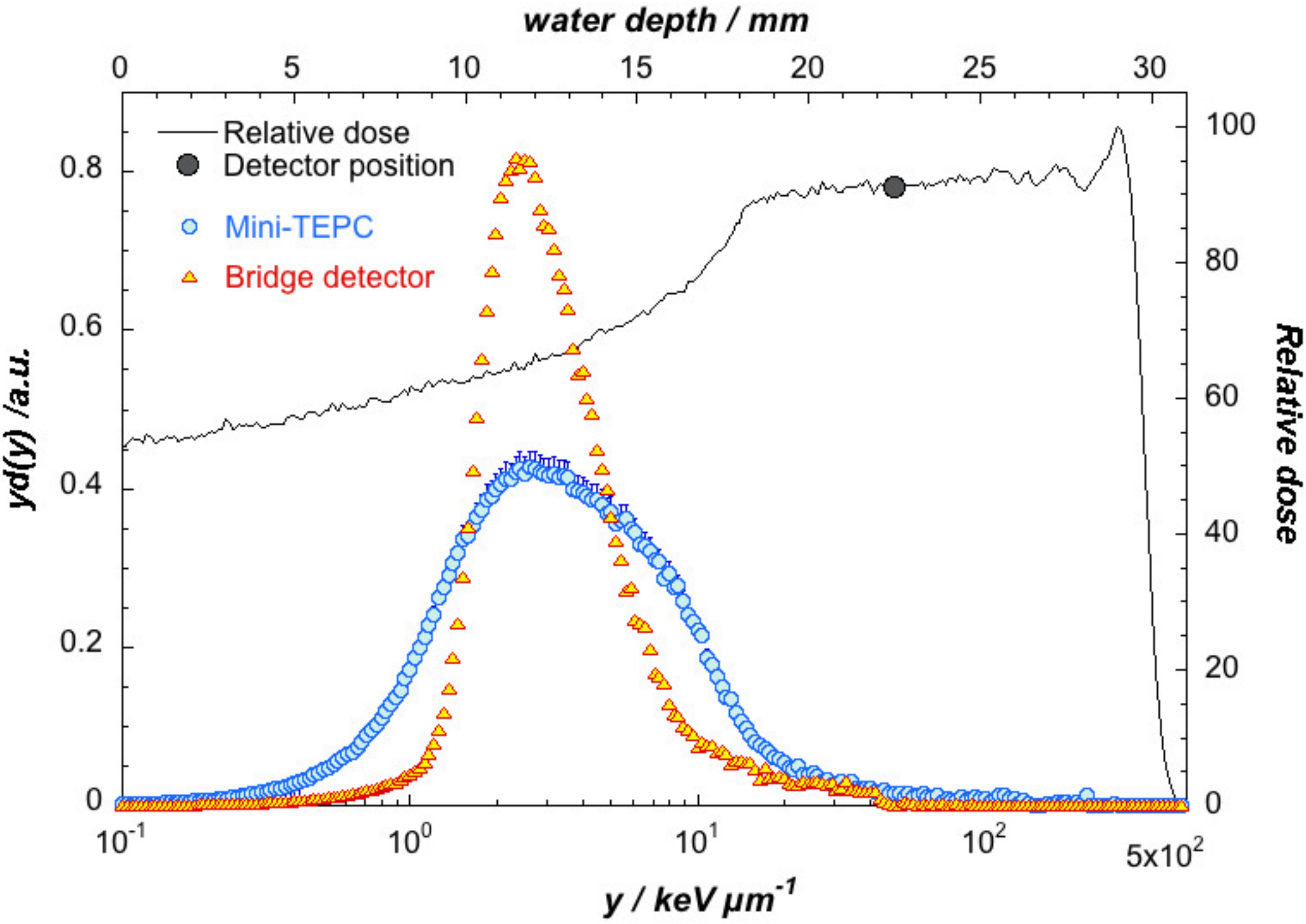
water depth / mm
0
5
10
15
20
25
30
Relative dose
Detector position
Mini-TEPC
Bridge detector
0.8
0.6
0.4
0.2
0
yd(y) /a.u.
100
80
60
40
20
0
Relative dose
10^{-1}
10^{0}
10^{1}
10^{2}
$5x10^{2}$
y / keV µm^{-1}

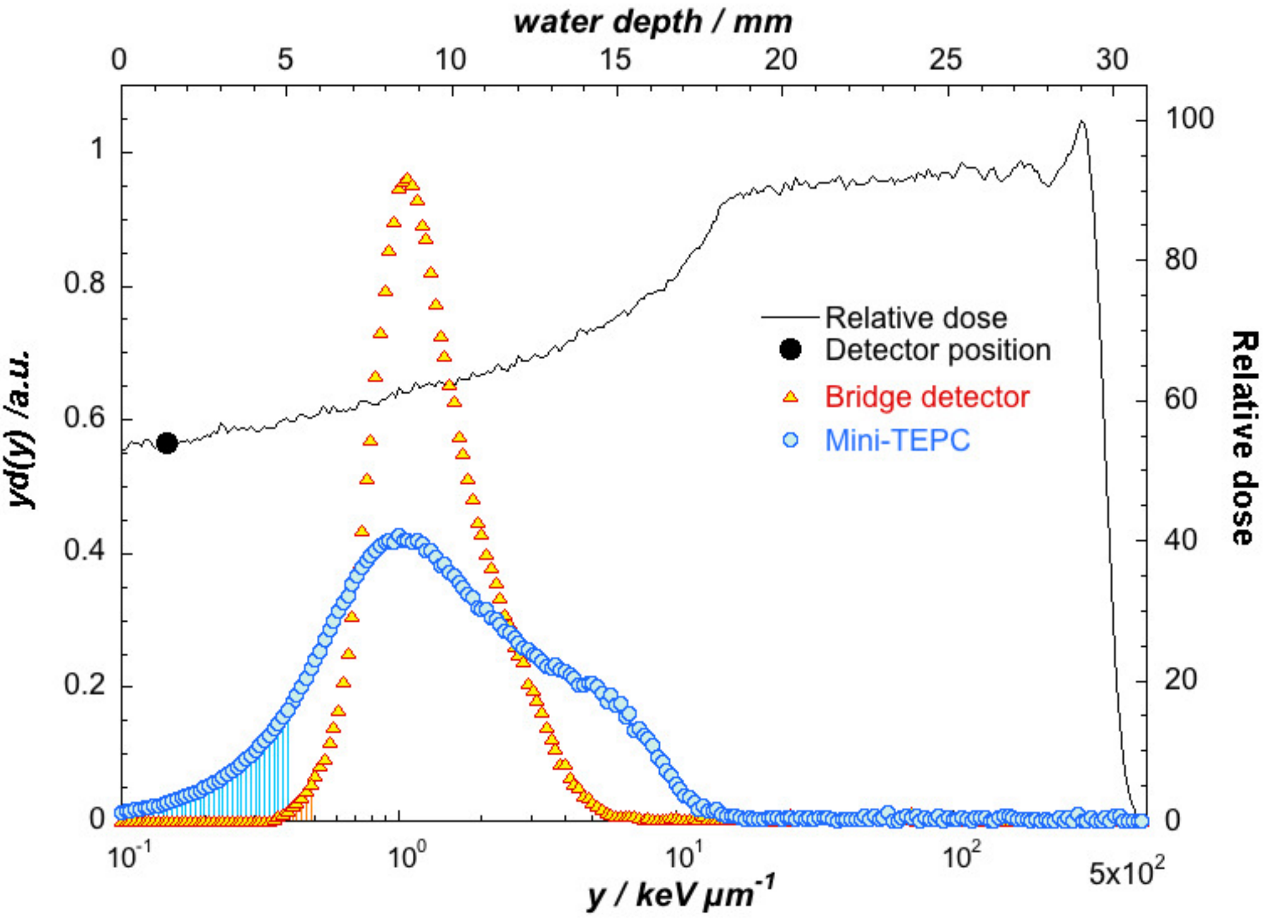
water depth / mm
0
5
10
15
20
25
30
1
0.8
0.6
0.4
0.2
0
yd(y) /a.u.
100
80
60
40
20
0
Relative dose
Relative dose
Detector position
Bridge detector
Mini-TEPC
10^-1
10^0
10^1
10^2
5x10^2
y / keV µm^-1

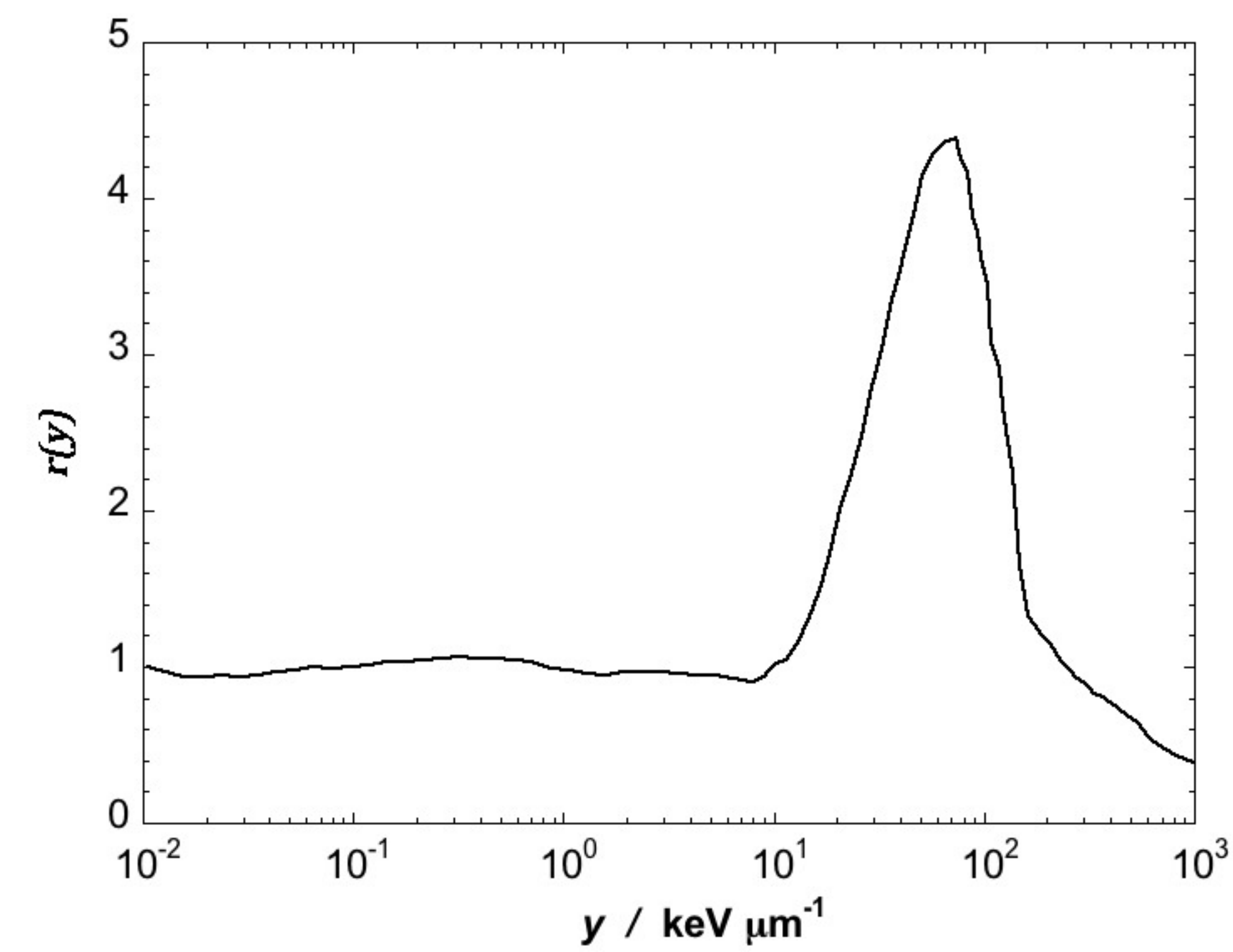
r(y)
0
1
2
3
4
5
10-2
10-1
100
101
102
103
y / keV μm-1

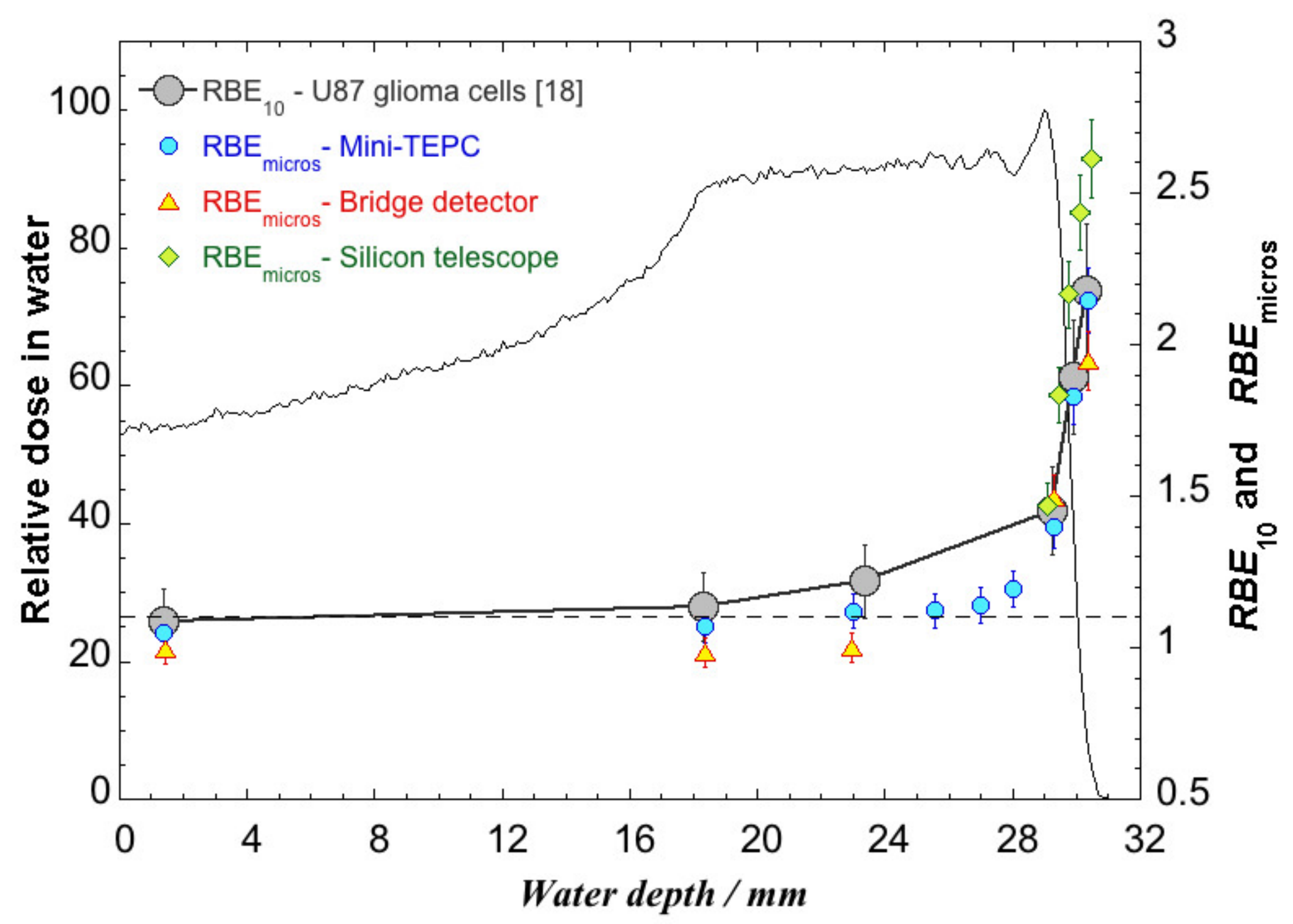
RBE10 - U87 glioma cells [18]
RBEmicros - Mini-TEPC
RBEmicros - Bridge detector
RBEmicros - Silicon telescope
Relative dose in water
RBE10 and RBEmicros
Water depth / mm
0
20
40
60
80
100
0.5
1
1.5
2
2.5
3
0
4
8
12
16
20
24
28
32